

**Chaotic advection in a three-dimensional
time-dependent system**

by

J. F. Adams

A thesis submitted to the
Faculty of the Graduate School of the
University of Colorado in partial fulfillment
of the requirements for the degree of
Master of Science
Department of Applied Mathematics
2010

This thesis entitled:
Chaotic advection in a three-dimensional time-dependent system
written by J. F. Adams
has been approved for the Department of Applied Mathematics

Dr. James Meiss

Dr. James Curry

Dr. Robert Easton

Date _____

The final copy of this thesis has been examined by the signatories, and we find that both the content and the form meet acceptable presentation standards of scholarly work in the above mentioned discipline.

Adams, J. F. (M.S., Applied Mathematics)

Chaotic advection in a three-dimensional time-dependent system

Thesis directed by Dr. James Meiss

In certain systems, fluid elements can exhibit a chaotic trajectory. This is termed Chaotic Advection, and has potential applications in fluid-mixing problems where creating a turbulent flow is unreasonable. This thesis generalizes a famous system, Hassan Aref's Blinking Vortex model, and analyzes the flow with both numerical simulations and physical experiments.

The model is a three-dimensional, time-dependent, inviscid, irrotational and incompressible flow bounded by the unit cube. The velocity field is generated by alternating between two different vortex tubes that pass through the cube with the axis of the tube parallel to one of the Cartesian axes. To create the boundary, it is necessary to use a lattice of point vortices via the method of images in the complex plane.

Simulations show evidence of torus-like structure under certain schemes, and a breakdown of structure (possibly chaos) in other schemes. Physical experimentation shows some characteristics of the model are preserved, where others are lost due to real-world attributes like viscosity.

Dedication

To my dog, Grizzly.

Acknowledgements

For providing excellent advice and guidance, I must thank: Jim Meiss, Anne Dougherty, Jim Curry. Without these mentors, I would be much less off. For being on my committee, I thank Jim Meiss, Jim Curry and Bob Easton. For offering academic support and friendship, I must recognize Ryan Schilt and Jon Olsen. For being supportive in all other ways, I must mention: Mom, Dad, Jess, Shannon, Andy, Steve.

I also would like to recognize the Engineering Excellence Fund (EEF) which supported this project financially.

Contents

Chapter

1	Introduction	1
1.1	Historical Account of Chaotic Advection	2
1.2	Background Information	2
1.2.1	Eulerian and Lagrangian Flow	2
1.2.2	Existence of a Hamiltonian	3
1.3	The Blinking Vortex	4
1.3.1	Formulation of the Model	4
1.3.2	Piecewise-Constant Stirrer Motion	6
1.4	Blinking Rolls	8
1.4.1	Formulation of the Model	8
1.4.2	A Special Stream Function	10
2	Analytical Formulation of a Different Blinking Rolls Model	12
2.1	Vortex Lattice	13
2.1.1	A Single Vortex in the Complex Plane	13
2.1.2	Multiple Point-Vortices	13
2.2	Blinking Vortex Tubes	17
2.3	Continuous Vortex Tubes	18

3	Numerical Simulation	19
3.1	Development of Simulation	19
3.2	Intersection With a Two-Dimensional Plane	20
3.3	Trajectories	21
3.3.1	Restricted to a Torus	21
3.3.2	Chaotic Regime	21
4	Physical Experimentation	26
4.1	Experimental Set-up	26
4.1.1	The Boundary	26
4.1.2	The Vortex Tubes	26
4.1.3	The Fluid and Tracer	27
4.2	Experimental Results	27
5	Conclusions	32
5.1	What This Thesis Did	32
5.2	What I Would Do Differently	32
5.3	Future Work	33
Bibliography		34
Appendix		
A	Simulation Code	35
A.1	Plane-Intersection	35
A.2	Particle Trajectory	38
B	Microcontroller Code	41

Tables

Table

Figures

Figure

1.1 Streamlines of the flow given H as described by (1.7) when $z(t) = b = \frac{1}{2}$ and $a = 1$. The bold circle is both a streamline and the boundary.	5
1.2 Example of the flow of a roll when $\psi_1(y, z)$ has positive rotation about the x axis[5].	9
1.3 Streamlines of the flow given ψ_x as described by (1.24)	10
2.1 This is the set-up for a new system of blinking rolls. The bold lines represent the locations of two vortex-tubes. In this case the vortex tubes do not intersect.	12
2.2 Streamlines for ten vortices in random locations with random strengths.	14
2.3 A lattice configuration to create square boundaries.	15
2.4 The square boundary of the first vortex.	15
2.5 Streamlines with directions as given by (2.15) with $a = b = 2/5$ and $\Gamma = 2\pi$	17
3.1 This figure shows the location of the plane. Notice how it is directly between the two rolls and does not intersect with them.	22
3.2 In this figure, $\mu = 0.01$ and the initial condition is $\mathbf{x}_0 = (0.5, 0.5, 0.5)$. Each dot represents where the element crossed the plane. Notice the big holes where the element never enters.	22

3.3	In this figure, $\mu = 0.01$ again, but the initial starting point is within one of the holes from figure 3.2 ($\mathbf{x}_0 = (0.2, 0.5, 0.4)$). This image is evidence that there is some underlying structure, like invariant tori.	23
3.4	In this figure, $\mu = 0.005$ and $\mathbf{x}_0 = (0.5, 0.5, 0.5)$. See how the gaps have gotten bigger.	23
3.5	In this figure, $\mu = 0.02$ and $\mathbf{x}_0 = (0.5, 0.5, 0.5)$. Now there are no gaps. .	24
3.6	In this figure, $\mu = 0.01$. The blue path is the trajectory of the single element with initial condition $\mathbf{x}_0 = (0.2, 0.5, 0.4)$, which is the same scheme used in figure 3.3	24
3.7	In this figure, $\mu = 0.025$ and $\mathbf{x}_0 = (0.5, 0.5, 0.5)$. The blue path is again the trajectory of the single initial element.	25
4.1	This is a good view of the overall set-up.	28
4.2	Another angle of view.	28
4.3	Another angle of view with both rods continuously running.	28
4.4	Here is the beginning of another experiment with $\mu = 10$	29
4.5	A different angle of figure 4.4.	29
4.6	A little while later with $\mu = 10$	29
4.7	$\mu = 10$ like 4.6 but from the side.	30
4.8	Again with $\mu = 10$ a little bit later.	30
4.9	The same as 4.8 but from the side.	30
4.10	A little bit later with $\mu = 10$	31
4.11	A comparison of the numerical simulation and the physical experiment. Notice how in both cases the tracer spirals around the vortex tubes. . .	31

Chapter 1

Introduction

When a small fluid element moves with the local fluid velocity, we say it is *advected* through the system. The element's movement is considered passive, meaning it doesn't affect other fluid elements. All it is able to do is follow the fluid around it, adjusting its velocity to the surrounding flow. Following this single fluid element is often termed the *Lagrangian* method of viewing fluid mechanics. Its counterpart is the *Eulerian* method, which involves using entire fields (or control volumes) rather than individual elements.

Within the field of dynamical systems, *chaos* has several different characteristics attributed to it, including: aperiodic long-term behavior and sensitive dependence on initial conditions [8]. This means that if a system is chaotic, there are trajectories that do not settle down to a single point or a periodic orbit. It also means that nearby trajectories should separate exponentially fast.

Now, consider a fluid velocity field where the trajectories of individual elements behave like a chaotic system, i.e. chaotic fluid advection. Elements within regions of the system would, overtime, advect in aperiodic trajectories and would exponentially separate from nearby elements. This could lead to a well *mixed* fluid, even if everything is deterministic.

1.1 Historical Account of Chaotic Advection

The idea that a simple fluid system could exhibit chaotic behavior was certainly understood by the mid-1960's, but it wasn't until the early 1980's that the term *chaotic advection* came about [2]. In 1948, a paper by Carl Eckart gave an account on geophysical fluid dynamics. In his paper, Eckart defines the difference between *mixing* and *stirring*. He says, "...advection alone will ultimately increase the mean value of any initial gradient..." and: "This effect of advection is appropriately called stirring." He also writes: "The effect of conduction or diffusion is to decrease the mean value of the gradient. This is appropriately called mixing..." [2]. This is a nice definition of two terms that describe the mechanical and molecular physical processes that produce mixing.

In the mid-1960's, there were a couple of papers written by V. I. Arnol'd and M. Hénon that explored Beltrami flow, where velocity and vorticity are everywhere parallel. They reasoned that, in steady, inviscid flow, the fluid element paths could not be constrained to two-dimensional sheets, and would wander throughout a subset of the fluid volume [2].

The next milestone in the development of chaotic advection came in the early 1980's when Hassan Aref gave a talk titled "An idealized model of stirring" which was a presentation of the results of his famous "blinking vortex model." This is where the term *chaotic advection* most likely first arose in scientific literature [2]. Over the course of a few years, Aref's studies were published in several journals and interest in the subject was on the rise.

1.2 Background Information

1.2.1 Eulerian and Lagrangian Flow

There are two common schemes of analyzing fluid advection, the Eulerian and the Lagrangian perspectives. The Eulerian way of viewing flow is to describe the advected

property by a scalar field $\theta(\mathbf{x}, t)$ which will evolve through time and space in the form

$$\frac{\partial \theta}{\partial t} + \mathbf{u} \cdot \nabla \theta = \kappa \Delta \theta \quad (1.1)$$

Here θ is the scalar field, $\mathbf{u}(\mathbf{x}, t)$ is the velocity field, $\mathbf{x} = (x, y, z)$ is the spatial component, t is the temporal component and κ is a diffusivity constant. Although this equation is linear in θ , even simple flow fields can give rise to highly irregular and complex behavior.

The Lagrangian description of fluid advection is essentially to follow individual fluid elements. This is done with the following system of equations

$$\dot{x} = u(x, y, z, t), \quad \dot{y} = v(x, y, z, t), \quad \dot{z} = w(x, y, z, t) \quad (1.2)$$

which are just the three components to the velocity field \mathbf{u} . The equations (1.2) are just a finite-dimensional dynamical system which are completely deterministic. Furthermore, if the fluid flow is steady (no time-dependence) then (1.2) is also autonomous.

1.2.2 Existence of a Hamiltonian

For the purpose of studying chaotic advection, the Lagrangian method will be employed. It is important to note that if the flow is steady, incompressible ($\nabla \cdot \mathbf{u} = 0$) and two-dimensional, then the advection problem (1.2) is integrable. Due to the incompressibility, there exists a stream function $\psi(x, y)$ whose contours are called streamlines. These streamlines happen to coincide with the pathlines of individual fluid elements when the flow is steady, meaning it is possible to find the trajectory of a given element. When the incompressibility is further examined, it is noticed that

$$\mathbf{u} = (\dot{x}, \dot{y}, \dot{z}) = \nabla \psi \times \hat{e}_z \quad (1.3)$$

which gives rise to

$$\dot{x} = -\frac{\partial \psi}{\partial y}, \quad \dot{y} = \frac{\partial \psi}{\partial x} \quad (1.4)$$

which are Hamilton's canonical equations for a system with one degree of freedom (which are also known to be integrable when autonomous). So, to take a Hamiltonian system into the realm of non-integrability, it is necessary to add a dimension (in space, time or both), which is exactly what Aref did in his Blinking Vortex analysis.

1.3 The Blinking Vortex

The Blinking Vortex model is simply a two-dimensional flow governed by a circular boundary and two point vortices that alternate between being “on” and “off”. The blinking of the vortices effectively takes an integrable, Hamiltonian system and turns it into a potentially chaotic map.

1.3.1 Formulation of the Model

The circular boundary of radius a will exist centered at the origin within the complex plane ($x + iy$). Rather than having two vortices, imagine one vortex that instantly changes position as a function of time, $z(t)$. This function is often referred to as the *stirring protocol*[1]. To create the circular boundary, it is necessary to create an image of the vortex at the position $a^2/\bar{z}(t)$. Note that this boundary has a “no flux” property which means fluid along the boundary always moves parallel to the boundary. This is also called a “free slip” boundary. The strength of the vortex is denoted by Γ , making the strength of its image $-\Gamma$ (same magnitude but in the opposite direction). This will completely generate the flow field.

Now consider an element of negligible mass at the position $\zeta(t)$. The equation of this element's motion is given by[1]

$$\dot{\zeta} = \frac{\Gamma}{2\pi i} \left\{ (\zeta - z)^{-1} - \left(\zeta - \frac{a^2}{\bar{z}} \right)^{-1} \right\} \quad (1.5)$$

This represents a non-autonomous system of two coupled, nonlinear, ordinary differential equations. The first term of (1.5) is the velocity field of the vortex at z and

the second term is of its image. There are several important results from the system generated by (1.5). *The system is a Hamiltonian* where if $\zeta = \xi + i\eta$ then

$$\dot{\xi} = -\frac{\partial H}{\partial \eta}, \quad \dot{\eta} = \frac{\partial H}{\partial \xi} \quad (1.6)$$

and

$$H = \frac{\Gamma}{2\pi} \log \left| \frac{\zeta - z}{\zeta - a^2/\bar{z}} \right| \quad (1.7)$$

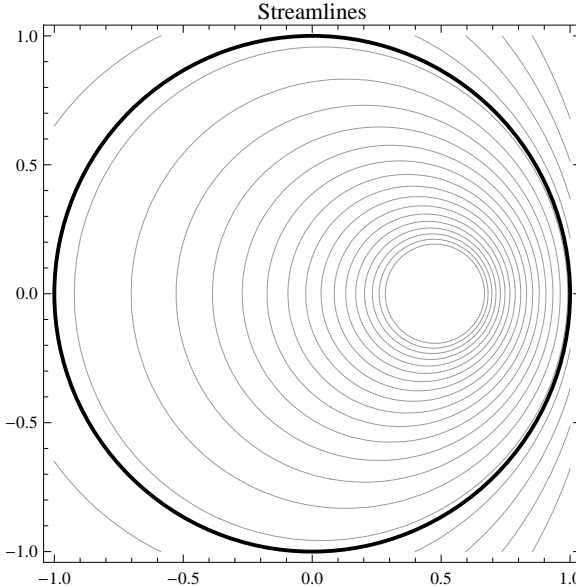


Figure 1.1: Streamlines of the flow given H as described by (1.7) when $z(t) = b = \frac{1}{2}$ and $a = 1$. The bold circle is both a streamline and the boundary.

The time- T flow at (1.6) generates an area-preserving map

$$M : \zeta(t) \rightarrow \zeta(t + T) \quad (1.8)$$

There are two known integrable cases: $z(t)$ is a constant or $z(t) = z_0 e^{i\Omega t}$. These results are all derived by Aref [1].

Now, rewrite the model using dimensionless variables. Let $z(t) = bf(t/T)$ where $b < a$ is a constant and f is a real, periodic function with period 1. This means that the vortex bounces back and forth between b and $-b$ according to function f . If we set $\zeta(t) = aZ(t/T)$ then $\zeta(t) = (a/T)Z'(t/T)$ where the prime denotes the derivative of Z .

Using the derivations of Aref [1] we end up with

$$\frac{d\bar{Z}}{d\tau} = i\mu \frac{1 - \beta^2 f^2}{(Z - \beta f)(\beta f Z - 1)} \quad (1.9)$$

where $\tau = t/T$ and

$$\beta = \frac{b}{a} \quad (1.10)$$

$$\mu = \frac{\Gamma T}{2\pi a^2} \quad (1.11)$$

1.3.2 Piecewise-Constant Stirrer Motion

Consider a vortex that bounces back and forth from b to $-b$ according to the period T in a piecewise-constant manner

$$z(t) = \begin{cases} +b & (nT \leq t < (n + \frac{1}{2})T) \\ -b & ((n + \frac{1}{2})T \leq t < (n + 1)T) \end{cases} \quad (1.12)$$

where $n = 0, \pm 1, \pm 2 \dots$, and b and T are constants.

While $0 \leq t < \frac{1}{2}T$ the element's motion is determined by [1]

$$\dot{\zeta} = \frac{\Gamma}{2\pi i} \frac{b^2 - a^2}{(\zeta - b)(b\zeta - a^2)} \quad (1.13)$$

which just means that it follows the arc of a circle given by H -constant from (1.7), or equivalently

$$\left| \frac{\zeta - b}{\zeta - a^2/b} \right| = \lambda \quad (1.14)$$

where λ is a constant between $0 < \lambda \leq b/a$ given by the initial position ζ_0 . The radius of this arc is given by

$$\rho = \frac{\lambda}{1 - \lambda^2} \left(\frac{a^2}{b} - b \right) \quad (1.15)$$

and its center can be determined to be

$$\zeta_c = \frac{b - \lambda^2 a^2/b}{1 - \lambda^2} \quad (1.16)$$

Now, substitute

$$\zeta = \zeta_c + \rho e^{i\phi} \quad (1.17)$$

into (1.13) and create an equation that describes the motion as related to ϕ

$$\dot{\phi} \left(1 - \frac{2\lambda}{1 - \lambda^2} \cos \phi \right) = \frac{\Gamma}{2\pi\rho^2} \frac{1 - \lambda^2}{1 + \lambda^2} \quad (1.18)$$

which can be integrated to obtain

$$\phi - \frac{2\lambda}{1 + \lambda^2} \sin \phi = \frac{\Gamma}{2\pi\rho^2} \frac{1 - \lambda^2}{1 + \lambda^2} (t - t_0) \quad (1.19)$$

where $\phi = 0$ when $t = t_0$. The left-hand side of (1.19), denoted by

$$A_\lambda(\phi) = \phi - \frac{2\lambda}{1 + \lambda^2} \sin \phi \quad (1.20)$$

is monotone since $\lambda < 1$, making a one-to-one correspondence with the angle ϕ through which the element has been revolved. This means that $A_\lambda(\phi) = \phi$ whenever $\phi = p\pi$ where $p = 0, \pm 1, \pm 2, \dots$. The *period of rotation* T_λ of the element can be discovered by

$$2\pi = \frac{\Gamma}{2\pi\rho^2} \frac{1 - \lambda^2}{1 + \lambda^2} T_\lambda \quad (1.21)$$

It is important to note that using the relationships in (1.15) and (1.18), it can be derived that

$$\Delta A_\lambda(\phi) = 2\pi \Delta t / T_\lambda \quad (1.22)$$

which tells the change in $A_\lambda(\phi)$ during a time interval Δt .

Now, we can determine the position of an advected element at time $t \leq \frac{1}{2}T$, denoted ζ_t , given its initial position ζ_0 . The algorithm is:

- STEP 1: Calculate λ from (1.14)
- STEP 2: Calculate ζ_c from (1.16)
- STEP 3: Calculate ρ and ϕ_0 from $\rho e^{i\phi_0} = \zeta_0 - \zeta_c$
- STEP 4: Calculate $A_\lambda(\phi_0)$ from (1.20)
- STEP 5: Calculate T_λ from (1.21)
- STEP 6: Calculate $A_\lambda(\phi_t) = A_\lambda(\phi_0) + 2\pi t / T_\lambda$
- STEP 7: Calculate ϕ_t using a root-finding method (Newton's Method) on $A_\lambda(\phi_t)$
- STEP 8: Calculate $\zeta_t = \zeta_c + \rho e^{i\phi_t}$

For the next half-period, $\frac{1}{2}T \leq t < T$, the vortex is at $-b$ and a similar calculation can be used to find ζ_T in terms of $\zeta_{\frac{1}{2}T}$. This algorithm, used to calculate the location

of elements every half-period, has been implemented and the simulation can be found at <http://appmsaga.colorado.edu/>. The simulation uses $\beta = 0.5$ and allows the user to choose the value of μ .

1.4 Blinking Rolls

In this section we introduce a three-dimensional extension of Aref's Blinking Vortex that we call "Blinking Rolls" [5]. Rather than having a point-vortex bouncing back and forth within a circular boundary, imagine a pair of vortex-tubes, or *rolls*, that exist within a cubic boundary and alternate being "on" and "off" according to some period. These rolls travel directly through the center of opposite sides of the cube, and thus intersect each other in the very center at a 90 degree angle. Note that there will be no *drift* along the axis of the roll that is currently agitating the flow. This means the flow field can be represented in terms of a stream function ψ by

$$\mathbf{v} = \nabla\psi(\mathbf{x}_\perp, t) \times \hat{\mathbf{e}}_{||} \quad (1.23)$$

where $\hat{\mathbf{e}}_{||}$ is a unit vector in the invariant direction (along the axis of the current roll). This restricts the motion to the \mathbf{x}_\perp plane. Furthermore, if ψ is autonomous, then the motion is confined to a two-dimensional surface defined by ψ constant [5].

1.4.1 Formulation of the Model

The study of [5] is primarily concerned when the rolls are *trigonometric*, meaning if the roll is aligned in the x direction, the stream function is given by

$$\psi = A \cos(y) \cos(z) \quad (1.24)$$

giving the velocity field

$$(\dot{x}, \dot{y}, \dot{z}) = \nabla\psi(y, z) \times \hat{\mathbf{e}}_x = (0, -A \cos(y) \sin(z), A \sin(y) \cos(z)) \quad (1.25)$$

Note that the value of A is analogous to the vortex strength Γ in Aref's model. The path that an element follows (i.e. the shape of streamlines, when ψ is constant) is a topological circle that limits to a square as you approach the boundary. The line $(y, z) = (\frac{\pi}{2}, \frac{\pi}{2})$ corresponds to a saddle equilibria.

To generalize the vortex-tube to all three directions within the cube, the following velocity field is created:

$$\mathbf{v}(\mathbf{x}, t) = A(t)\nabla\psi_1 \times \hat{\mathbf{e}}_1 + B(t)\nabla\psi_2 \times \hat{\mathbf{e}}_2 + C(t)\nabla\psi_3 \times \hat{\mathbf{e}}_3 \quad (1.26)$$

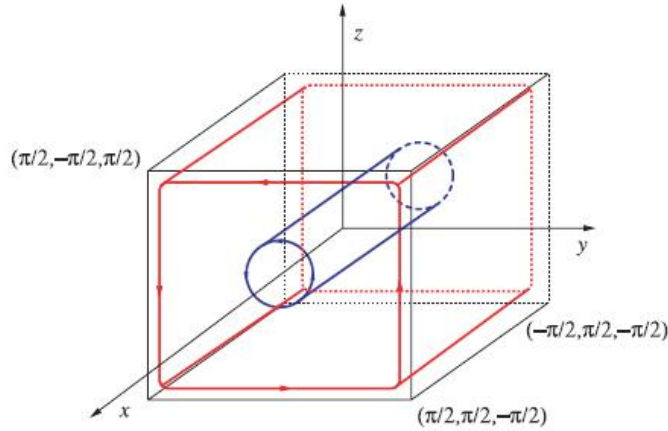


Figure 1.2: Example of the flow of a roll when $\psi_1(y, z)$ has positive rotation about the x axis[5].

When $A(t)$, $B(t)$ and $C(t)$ are chosen arbitrarily, it is presumably impossible to explicitly solve for the flow[5]. For the case of *blinking* rolls, these amplitude functions are alternating step functions. Furthermore, if the ψ_i 's are fixed, then there are six parameters; T_1 , T_2 , T_3 and A , B , C .

Since the rolls are blinking, there is only one vortex active at a time, meaning if we can obtain an explicit solution for the flow of a given ψ_i then an explicit time- t map can be created during the period T_i . The time- T_i map of the stream function ψ_i is

denoted

$$F_i(x, y, z) = \Phi_{T_i}(x, y, z), \quad \frac{d}{dt}\Phi_t = v_i(\Phi_t), \quad \Phi_0 = id. \quad (1.27)$$

where i represents one of three directions. The blinking roll map is subsequently the composition of these maps:

$$(x', y', z') = F_1 \circ F_2 \circ F_3(x, y, z) \quad (1.28)$$

Next, consider what happens when ψ is like that in (1.24).

1.4.2 A Special Stream Function

We begin by constructing the three-dimensional map for the velocity field described by (1.26), rolls (1.24) and amplitudes that are alternating step functions. The process starts with analyzing the flow for a single roll, then constructing the composition of the three maps to obtain (1.28).

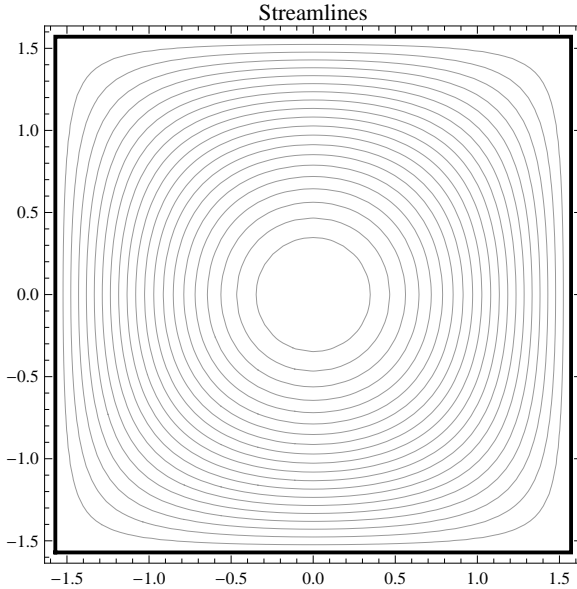


Figure 1.3: Streamlines of the flow given ψ_x as described by (1.24)

The solution to the differential equations (1.25) is obtained by noticing the tra-

jectories must satisfy $\frac{dy}{v_2} = \frac{dz}{v_3}$, giving rise to the Jacobi elliptic functions and producing

$$\Phi_t \begin{pmatrix} x \\ y \\ z \end{pmatrix} = \begin{pmatrix} x \\ \sin^{-1}(k \mathbf{sn}(At - M(y, z), k)) \\ \sin^{-1}(k \mathbf{sn}(At + N(y, z), k)) \end{pmatrix} \quad (1.29)$$

where the elliptic function has modulus

$$k = \sqrt{1 - \cos^2(y) \cos^2(z)}. \quad (1.30)$$

After scaling and simplification using methods in the Mullowney et al paper[5], the flow becomes:

$$\Phi_T \begin{pmatrix} x \\ y \\ z \end{pmatrix} = \begin{pmatrix} x \\ \sin^{-1}\left(\frac{\sin(y)\mathbf{cn}(T)\mathbf{dn}(T) - \mathbf{sn}(T)\sin(z)\cos^2(y)}{1 - \sin^2(y)\mathbf{sn}^2(T)}\right) \\ \sin^{-1}\left(\frac{\sin(z)\mathbf{cn}(T)\mathbf{dn}(T) + \mathbf{sn}(T)\sin(y)\cos^2(z)}{1 - \sin^2(z)\mathbf{sn}^2(T)}\right) \end{pmatrix} \quad (1.31)$$

From equation (1.31) the time- T_1 map becomes

$$F_1(x, y, z) = \Phi_{T_1}(x, y, z) \quad (1.32)$$

By rescaling time, the three amplitudes can be scaled so that $A = B = C = 1$, leaving only three parameters T_1 , T_2 and T_3 . The sign of each of the T_i 's represent the direction of rotation of the rolls. The paper written by Mullowney, Meiss and Julien continues on to show that an invariant exists under these conditions[5].

Chapter 2

Analytical Formulation of a Different Blinking Rolls Model

This chapter deals with the analytical derivation for the following set-up:

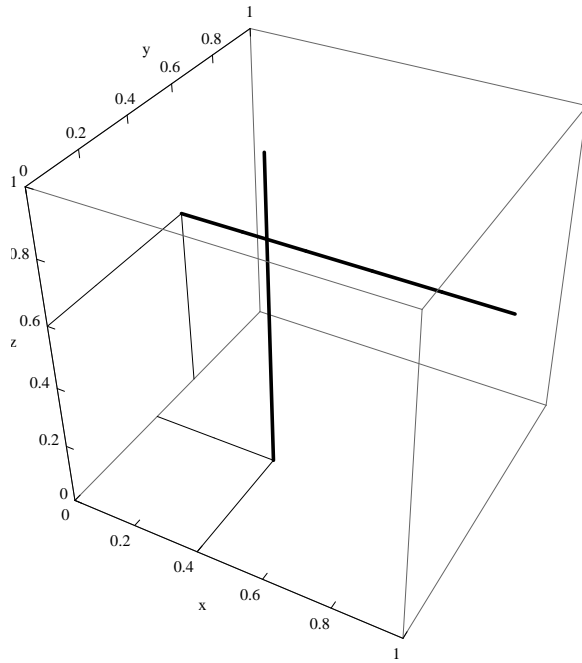


Figure 2.1: This is the set-up for a new system of blinking rolls. The bold lines represent the locations of two vortex-tubes. In this case the vortex tubes do not intersect.

As seen in figure 2.1, there are vortex-tubes, or rolls, that exist in a cubic domain.

These rolls do not necessarily have to intersect, and similar to the blinking rolls from the previous chapter, they alternate being “on” and “off”. This produces a volume preserving map that is analogous to fluid rotating around the rolls held within a cubic, no-flux boundary.

2.1 Vortex Lattice

2.1.1 A Single Vortex in the Complex Plane

When studying a point-vortex in two dimensions, it is very common to consider the *irrotational vortex* in the complex plane. This is fully described by the *complex potential* function

$$w(z) = \frac{\Gamma}{2\pi i} \ln(z) \quad (2.1)$$

where Γ is the strength of the vortex, which is located at the origin[3]. From this complex potential function, the real and imaginary parts give rise to the *velocity potential* and the *stream function* by $w = \phi + i\psi$

$$\phi = \frac{\Gamma}{2\pi} \theta, \quad \psi = -\frac{\Gamma}{2\pi} \ln(\rho) \quad (2.2)$$

where $\rho = |z|$ and $\theta = \arg(z)$ using a polar transformation $z = \rho e^{i\theta}$. The velocity can then be derived by

$$\mathbf{u} = \frac{dw}{dz} \quad (2.3)$$

meaning[3]

$$u_\rho = 0, \quad u_\theta = \frac{\Gamma}{2\pi\rho} \quad (2.4)$$

From (2.4), it is seen that there is zero velocity in the radial direction, and the tangential velocity drops off as $1/\rho$.

2.1.2 Multiple Point-Vortices

When multiple vortices exist, deriving the flow is simply a matter of superposition.

Using (2.1) for N vortices at locations $r_j, j = 1, 2, \dots, N$, the complex potential becomes

$$w(z) = \frac{1}{2\pi i} \sum_{j=1}^N \Gamma_j \ln(z - r_j) \quad (2.5)$$

giving rise to the velocity equation

$$\frac{dw}{dz} = u_{x_1} - iu_{x_2} = \frac{1}{2\pi i} \sum_{j=1}^N \frac{\Gamma_j}{z - r_j} \quad (2.6)$$

where u_{x_1} and u_{x_2} are the velocity components in the x_1 and x_2 directions. Figure 2.2 shows streamlines from ten point vortices superposed together.

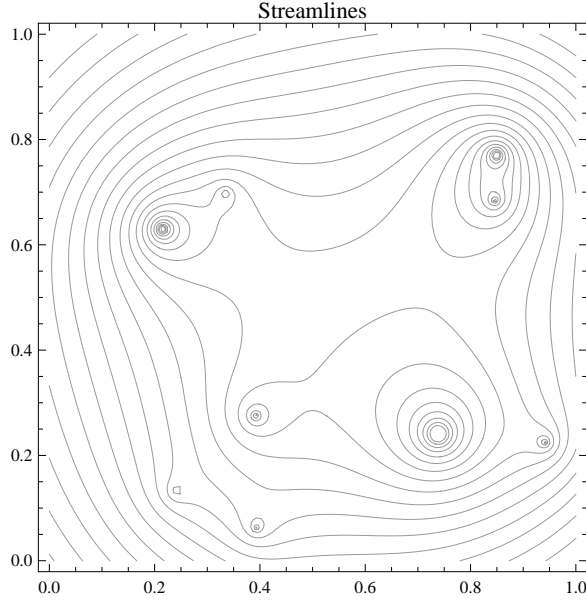


Figure 2.2: Streamlines for ten vortices in random locations with random strengths.

In order to create a square boundary for an off-center vortex, it is necessary to take an infinite number of vortex images and superpose them[6]. The positions and strengths of these images abide by a pattern that is graphically shown in Figure 2.3.

As shown in Figure 2.3, the direction of the vortex images alternates in the x_1 and x_2 directions. The magnitude of the strengths of these vortices are the same, meaning $\Gamma_{j,k} = -\Gamma_{j+1,k}$ where the indices j, k represent the vortex images in the x_1 and x_2 directions respectively.

$$\Gamma_{j,k} = \begin{cases} \Gamma & \text{for } j\text{-odd, } k\text{-odd} \\ -\Gamma & \text{for } j\text{-odd, } k\text{-even} \\ -\Gamma & \text{for } j\text{-even, } k\text{-odd} \\ \Gamma & \text{for } j\text{-even, } k\text{-even} \end{cases} \quad (2.7)$$

To simplify things, assume the square boundary has edges of length one. Fur-

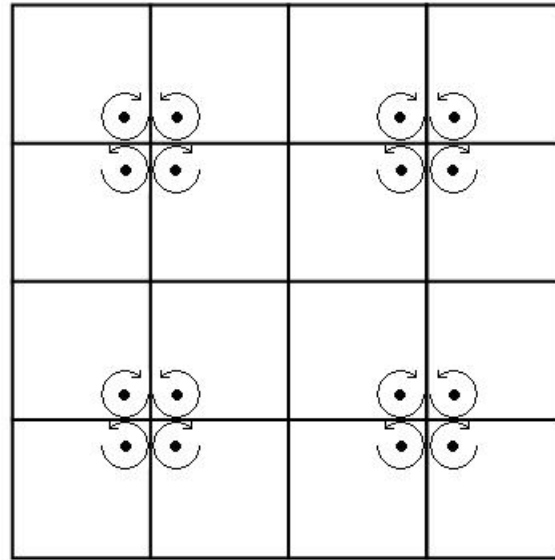


Figure 2.3: A lattice configuration to create square boundaries.

thermore, let the position of the vortex within the boundary be denoted

$$r_{1,1} = a + bi \quad (2.8)$$

where clearly $0 < a, b < 1$. Figure 2.4 shows a graphical representation of this.

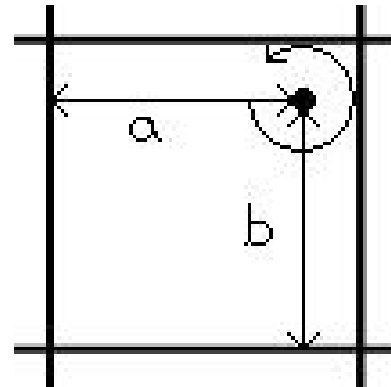


Figure 2.4: The square boundary of the first vortex.

This gives rise to a formula for the position of each vortex:

$$r_{j,k} = \begin{cases} (j-1+a) + i(k-1+b) & \text{for } j\text{-odd, } k\text{-odd} \\ (j-1+a) + i(k-b) & \text{for } j\text{-odd, } k\text{-even} \\ (j-a) + i(k-1+b) & \text{for } j\text{-even, } k\text{-odd} \\ (j-a) + i(k-b) & \text{for } j\text{-even, } k\text{-even} \end{cases} \quad (2.9)$$

Given this information, it is tempting to simply take the limit as $N \rightarrow \infty$ in equation (2.5) (and renumber the indices to match $r_{j,k}$), producing

$$w(z) = \frac{1}{2\pi i} \sum_{j,k=-\infty}^{+\infty} \Gamma_{j,k} \ln(z - r_{j,k})$$

However, this sum will not converge, nor will the same extension for equation 2.6.

$$\frac{dw}{dz} = u_{x_1} - iu_{x_2} = \frac{1}{2\pi i} \sum_{j,k=-\infty}^{+\infty} \frac{\Gamma_{j,k}}{z - r_{j,k}}$$

In order to produce a velocity field for this lattice, it is necessary to turn to the *Weierstrass zeta function*.

$$\zeta(z; \omega_1, \omega_2) = \frac{1}{z} + \sum_{n,m=-\infty}^{+\infty} \left(\frac{1}{z - \Omega_{n,m}} + \frac{1}{\Omega_{n,m}} + \frac{z}{\Omega_{n,m}^2} \right), \quad n \neq 0, m \neq 0 \quad (2.10)$$

where $\Omega_{n,m} = 2n\omega_1 + 2m\omega_2$, with ω_1 and ω_2 the *elliptic invariants*. Combining (2.10) with (2.9) and (2.7), we end up with a function for the velocity field we want. First define the following:

$$\zeta_1(z) = \zeta(z - (a + ib); \omega_1, \omega_2) \quad (2.11)$$

$$\zeta_2(z) = \zeta(z - (2 - a + ib); \omega_1, \omega_2) \quad (2.12)$$

$$\zeta_3(z) = \zeta(z - (2 - a + i(2 - b)); \omega_1, \omega_2) \quad (2.13)$$

$$\zeta_4(z) = \zeta(z - (a + i(2 - b)); \omega_1, \omega_2) \quad (2.14)$$

where ω_1 and ω_2 are chosen to create a no-flux boundary along integer values of x_1 and x_2 ($\omega_1 = 11.817$ and $\omega_2 = 3.23712 \times 10^{-15}$). Now, superpose the ζ_i 's to create the full velocity field:

$$\frac{dw}{dz} = u_{x_1} - iu_{x_2} = \frac{\Gamma}{2\pi i} (\zeta_1(z) - \zeta_2(z) + \zeta_3(z) - \zeta_4(z)) \quad (2.15)$$

Plots of the streamlines for this velocity field are shown in Figure 2.5

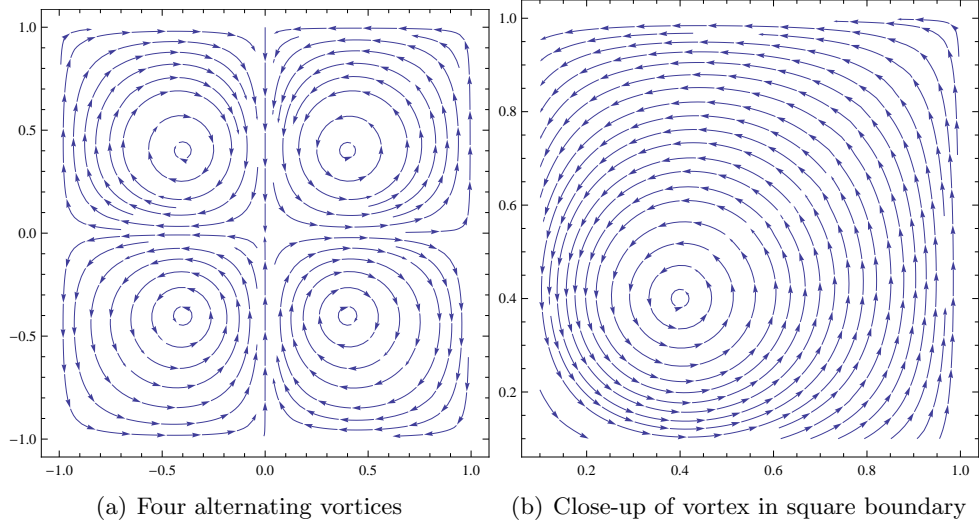


Figure 2.5: Streamlines with directions as given by (2.15) with $a = b = 2/5$ and $\Gamma = 2\pi$

2.2 Blinking Vortex Tubes

Now that equation (2.15) gives us a velocity field, the extension to blinking vortices is identical to what was done in the previous chapter. For the field of a vortex tube that is running parallel to the x_3 axis, the following system of differential equations describes the flow.

$$\begin{pmatrix} \dot{x}_1 \\ \dot{x}_2 \\ \dot{x}_3 \end{pmatrix} = \begin{pmatrix} Re[\frac{dw}{dz}] \\ -Im[\frac{dw}{dz}] \\ 0 \end{pmatrix} \quad (2.16)$$

where $\frac{dw}{dz}$ is like that in (2.15) and $z = x_1 + ix_2$. This means, for $0 < t < T$, we can integrate to find $(x_1(t), x_2(t), x_3(t))$ with T the *period* of the flow, or the length of time that a given vortex tube is agitating the fluid. The solution to the system in (2.16) is denoted

$$F_{x_1}(\mathbf{x}, t) \quad (2.17)$$

with $F_{x_3}(\mathbf{x}, t)$ similarly defined for a vortex tube parallel to the x_3 axis. Just like the previous chapter, a composition of maps will generate the overall mapping of particles

in the flow.

$$F_T(\mathbf{x}) = F_{x_1}(\mathbf{x}, T) \circ F_{x_3}(\mathbf{x}, T) \quad (2.18)$$

This is, of course, assuming there are only two vortex tubes operating in the x_1 and x_3 directions. It is not necessary to be restricted to this case, and the map is easily modified by adding more solutions to the system (2.16) for differing values of a , b , Γ , etc. The next chapter shows some of the numerical results of a specific example.

2.3 Continuous Vortex Tubes

Having a blinking vortex map is not necessary with the analytical derivation given above. Since the system is autonomous, it is easy to represent the case where multiple vortex tubes are continuously running. All that is required is to add the velocity fields together, i.e.

$$\dot{\mathbf{x}} = \sum_n (\mathbf{u}_n) \quad (2.19)$$

which then makes the solution simply

$$\mathbf{x}(t) = \sum_n (\mathbf{F}_n(\mathbf{x}, t)) \quad (2.20)$$

Chapter 3

Numerical Simulation

One component of the analysis for the model created in the previous chapter is to create a numerical simulation. What follows is an account of the creation and experimentation of a simulation modeled for a cube with two vortex tubes alternating “on” and “off”. These tubes travel through the cube parallel to the x_1 and x_3 axes, intersecting the sides of the cube at specific locations as discussed below.

3.1 Development of Simulation

The first step is to non-dimensionalize the formulation from the previous chapter. For this, consider that the length of one edge of the cube was set to be unity, $L = 1$, so that

$$\alpha = \frac{a}{L} = a, \quad \beta = \frac{b}{L} = b \quad (3.1)$$

Next, there needs to be a relation between the vortex strength, Γ , and the period, T . This is all under the assumption that each vortex tube has the same strength and operates for the same amount of time. We define

$$\mu = \frac{\Gamma T}{2\pi L^2} \quad (3.2)$$

Now, a specific set-up is chosen for α and β for two blinking rolls. For vortex one, $\alpha_1 = \frac{2}{5}$ and $\beta_1 = \frac{2}{5}$. For vortex two, $\alpha_2 = \frac{3}{5}$ and $\beta_2 = \frac{3}{5}$. Vortex one will run parallel to the x_3 -axis, and vortex two will run parallel to the x_1 -axis, giving the following velocity

field:

$$\mathbf{V}_1(\mathbf{x}, t) = \begin{pmatrix} \dot{x}_1 \\ \dot{x}_2 \\ \dot{x}_3 \end{pmatrix} = \begin{pmatrix} Re[\frac{dw_1}{dz}] \\ -Im[\frac{dw_1}{dz}] \\ 0 \end{pmatrix}, \quad \mathbf{V}_2(\mathbf{x}, t) = \begin{pmatrix} \dot{x}_1 \\ \dot{x}_2 \\ \dot{x}_3 \end{pmatrix} = \begin{pmatrix} 0 \\ -Im[\frac{dw_2}{dz}] \\ Re[\frac{dw_2}{dz}] \end{pmatrix} \quad (3.3)$$

Making the assumption that vortex one starts, the map becomes

$$\mathbf{F}_T(\mathbf{x}) = \mathbf{F}_1(\mathbf{x}, T) \circ \mathbf{F}_2(\mathbf{x}, T) \quad (3.4)$$

where \mathbf{F}_i is the solution to \mathbf{V}_i at time $t = T$, making a *full* period (i.e. the time for each vortex to blink on/off once) equal to $2T$. For the remainder of this chapter, $\Gamma = 2\pi$ thus making $\mu = T$.

Now that there are nondimensional variables with a specific velocity field generated according to (3.3), the simulation can be created by solving the ODE. The code for this simulation, written in Mathematica, can be found in the appendix. The following sections use this simulation to run experiments.

3.2 Intersection With a Two-Dimensional Plane

One form of analysis is to plot where a given element crosses a plane within the cube. Simply imagine a plane cutting right between the two vortex tubes (see figure 3.1),

$$\left\{ (x, y, z) : 0 \leq x \leq 1, y = \frac{1}{2}, 0 \leq z \leq 1 \right\} \quad (3.5)$$

Then, given an initial starting location, follow the trajectory and put a dot on the plane where the element passes through. Figures 3.2, 3.3, 3.4 and 3.5 show some of the examples of this experiment.

Figures 3.2 and 3.3 give reason to believe that there is some underlying structure to the flow for $\mu = 0.01$. Figure 3.5, however, shows less evidence for structure when $\mu = 0.02$.

3.3 Trajectories

Now that there is reason to believe an underlying structure might exist, let's plot some of the trajectories from different schemes. All we do is run the simulation for a single initial condition and plot the path it follows.

3.3.1 Restricted to a Torus

Under certain conditions, the trajectories appear to be restricted to a torus, as seen in figure 3.6. It seems that for small values of μ this is the case, whereas when μ is large, there isn't much structure. From figure 3.6 you'll notice some "zig-zagging" or non-smooth behavior. This is from the blinking of the vortex tubes. Each *hard* angle is caused by the switching of one vortex to another.

3.3.2 Chaotic Regime

As stated above, when μ is large, there is generally a loss of structure. This makes the trajectory appear to be chaotic, as seen in figure 3.7, which is a good example of what looks like *aperiodic long-term behavior*. This is, however, not enough to *prove* chaos exists in this scheme. In order to be confident that chaos exists, it is necessary to study the sensitivity to initial conditions (i.e. find the Lyapunov exponents across the domain).

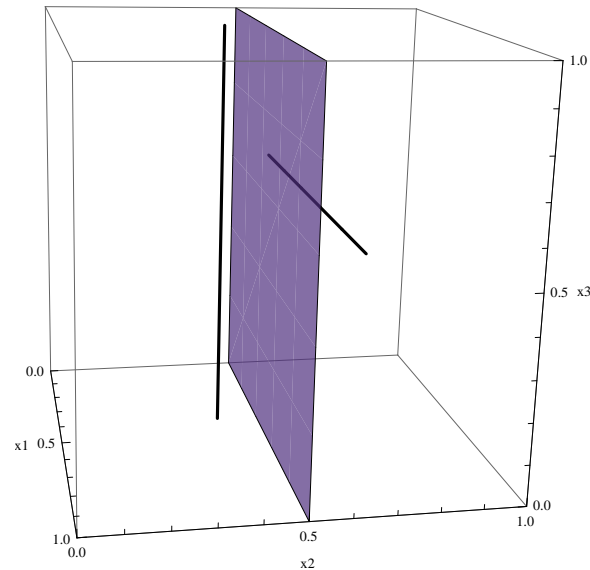


Figure 3.1: This figure shows the location of the plane. Notice how it is directly between the two rolls and does not intersect with them.

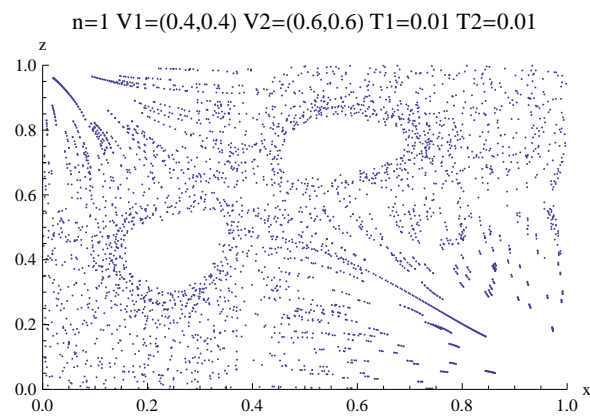


Figure 3.2: In this figure, $\mu = 0.01$ and the initial condition is $\mathbf{x}_0 = (0.5, 0.5, 0.5)$. Each dot represents where the element crossed the plane. Notice the big holes where the element never enters.

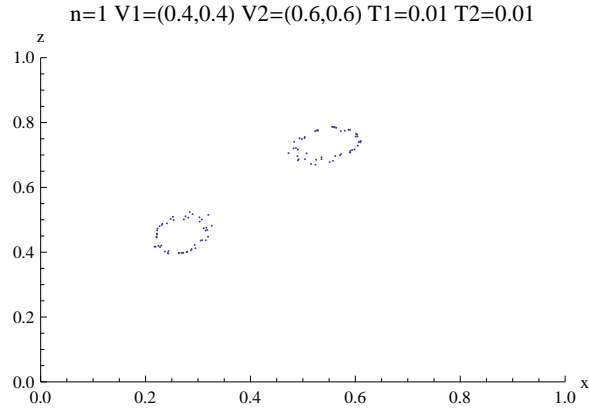


Figure 3.3: In this figure, $\mu = 0.01$ again, but the initial starting point is within one of the holes from figure 3.2 ($\mathbf{x}_0 = (0.2, 0.5, 0.4)$). This image is evidence that there is some underlying structure, like invariant tori.

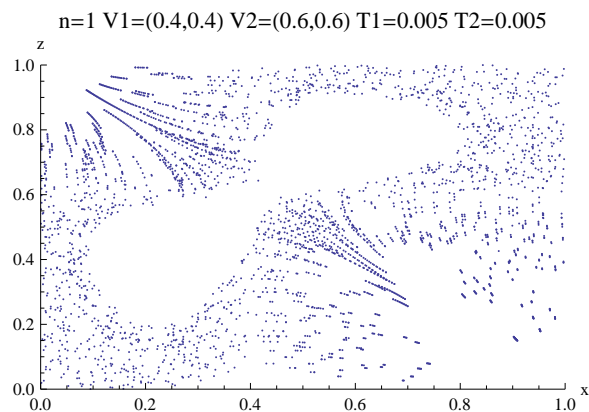


Figure 3.4: In this figure, $\mu = 0.005$ and $\mathbf{x}_0 = (0.5, 0.5, 0.5)$. See how the gaps have gotten bigger.

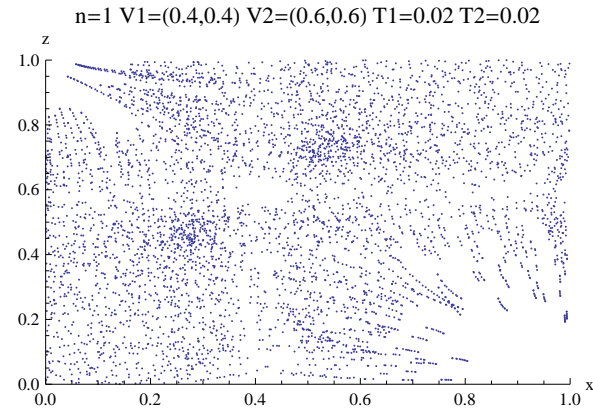


Figure 3.5: In this figure, $\mu = 0.02$ and $\mathbf{x}_0 = (0.5, 0.5, 0.5)$. Now there are no gaps.

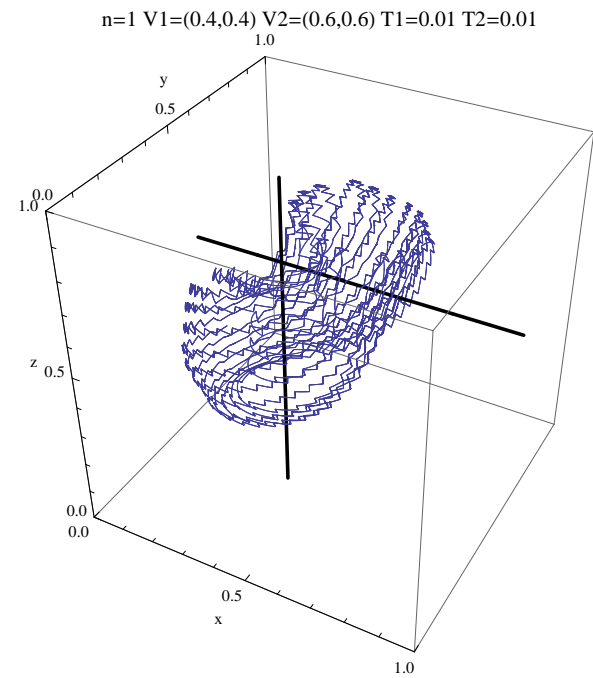


Figure 3.6: In this figure, $\mu = 0.01$. The blue path is the trajectory of the single element with initial condition $\mathbf{x}_0 = (0.2, 0.5, 0.4)$, which is the same scheme used in figure 3.3

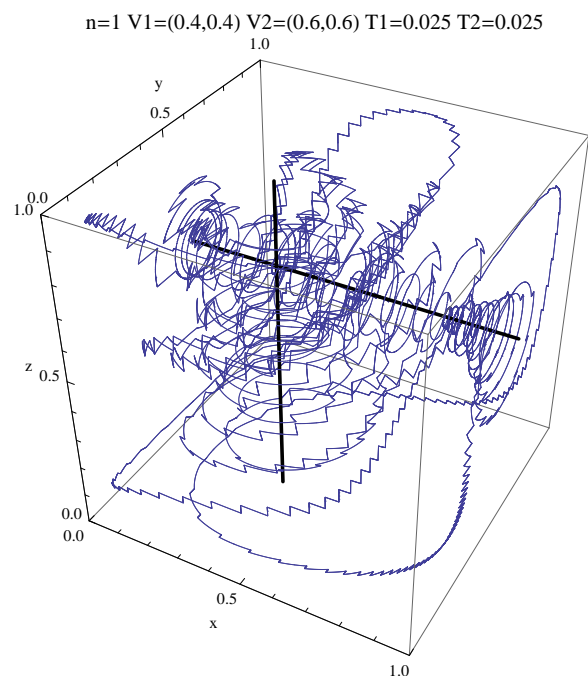


Figure 3.7: In this figure, $\mu = 0.025$ and $\mathbf{x}_0 = (0.5, 0.5, 0.5)$. The blue path is again the trajectory of the single initial element.

Chapter 4

Physical Experimentation

The last step in the analysis of the blinking vortex tubes is to create a physical apparatus that can conduct experiments. The numerical simulations from the previous chapter created some interesting images, but will the physical world do the same? What attributes of the idealized model will appear in a non-ideal realm? These questions are explored below.

4.1 Experimental Set-up

First, I need to recognize and thank the *Engineering Excellence Fund*. The monetary support that EEF gave me made this project possible.

4.1.1 The Boundary

The boundary of the cube is created using clear acrylic plastic. Each side of the cube is 8in. \times 8in. The base, however, is black acrylic and much larger (to accomodate the electronics described below). All of the plastic was purchased from Colorado Plastic Products, along with plastic adhesive used in the building process.

4.1.2 The Vortex Tubes

To create vortex tubes, two steel rods traversed the inside of the cube and were rotated. These rods were 5mm in diameter and 12in. long. At each juncture where the

rod passed through the boundary, a simple bearing was used to keep fluid from leaking out of the box and to reduce friction on the rod to allow it to spin. Both the rods and the bearings were purchased from McMaster-Carr. To rotate the rods, two stepper motors were used, with stepper motor drivers and a microcontroller. The motors were two-phase, four-wire stepper motors that were each connected to an EasyDriver V4.2 stepper motor driver. The drivers were connected to a microcontroller, the Arduino Duemilanove, which had a USB input from a computer (which uploaded the appropriate software to blink the rods). Each driver was hooked-up to a 9V DC power supply. The motors, drivers and microcontroller were all purchased from Sparkfun Electronics. The code for the Arduino is in the appendix.

4.1.3 The Fluid and Tracer

The fluid used for these experiments was clear glycerin from KIC Chemicals. The tracer dye was a combination of glycerin, red ink and blue food coloring. The dye was illuminated with a UV “black” light.

4.2 Experimental Results

What follows is a series of images showing the results of the physical experimentation:

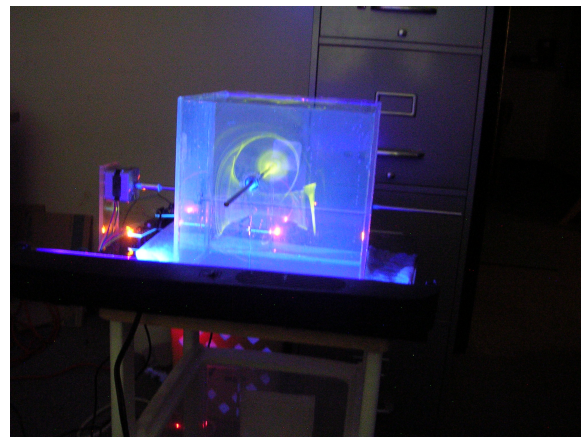


Figure 4.1: This is a good view of the overall set-up.

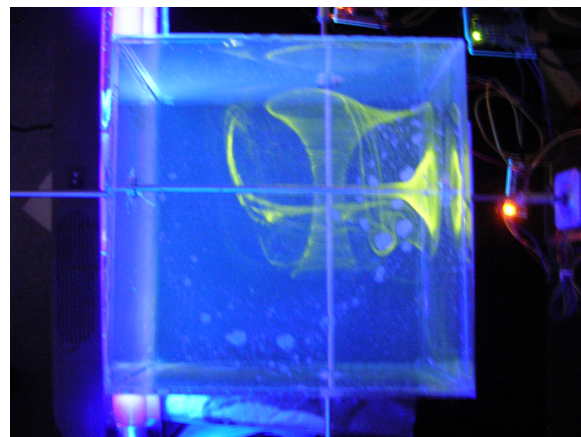


Figure 4.2: Another angle of view.

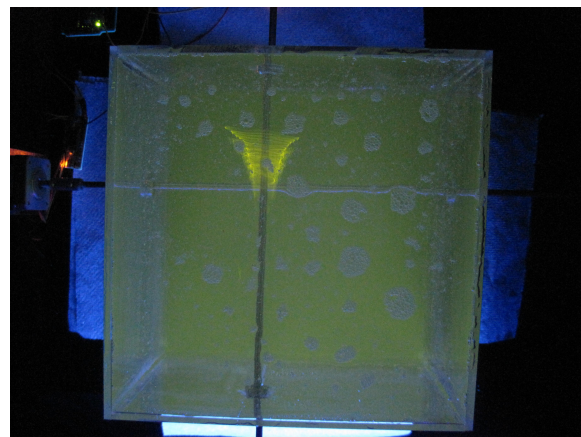


Figure 4.3: Another angle of view with both rods continuously running.

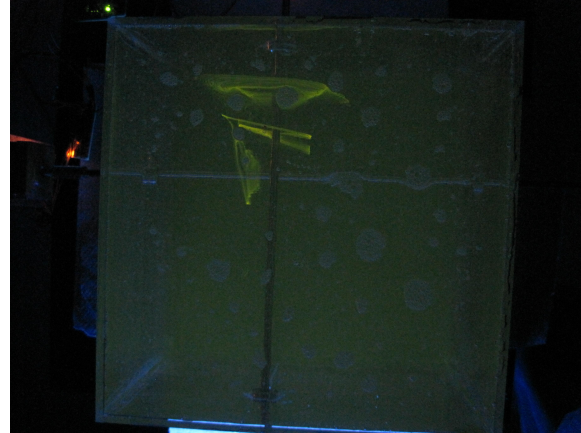


Figure 4.4: Here is the beginning of another experiment with $\mu = 10$.

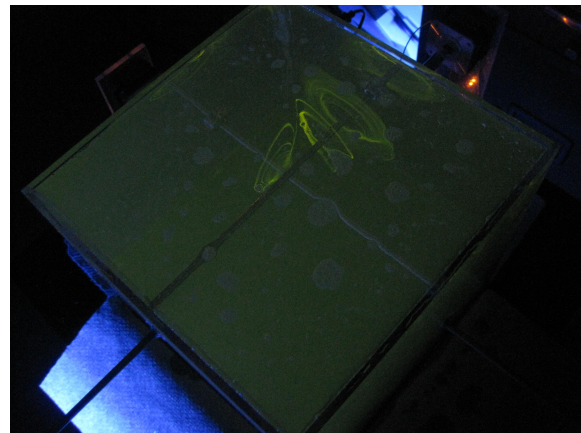


Figure 4.5: A different angle of figure 4.4.

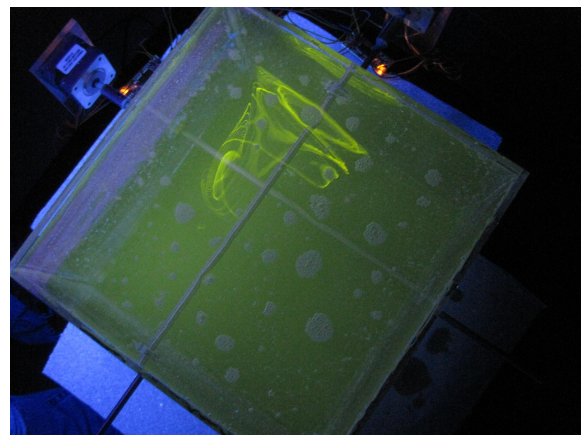


Figure 4.6: A little while later with $\mu = 10$

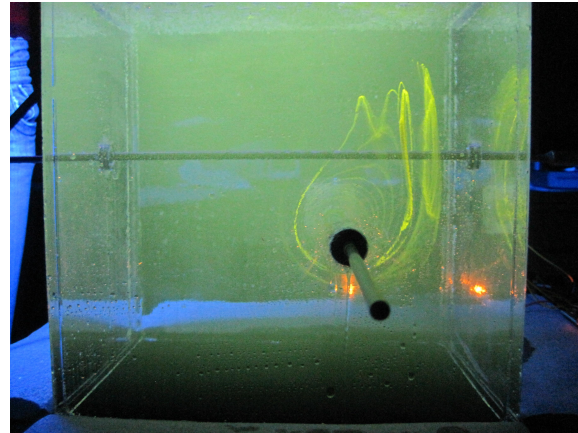


Figure 4.7: $\mu = 10$ like 4.6 but from the side.

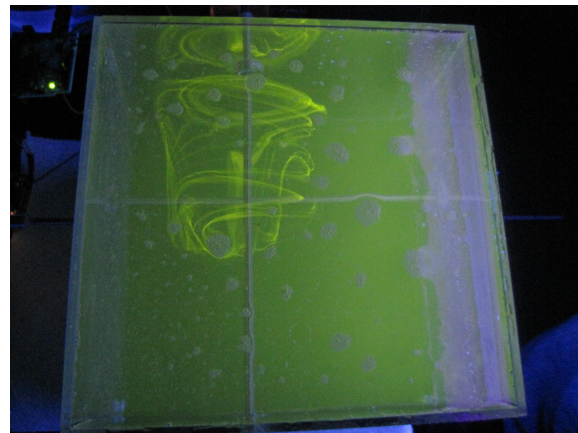


Figure 4.8: Again with $\mu = 10$ a little bit later.

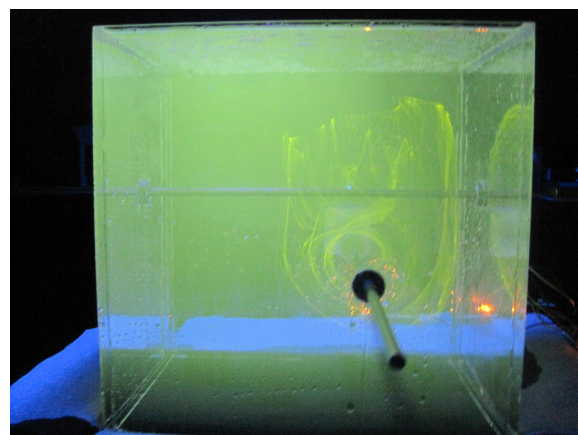


Figure 4.9: The same as 4.8 but from the side.

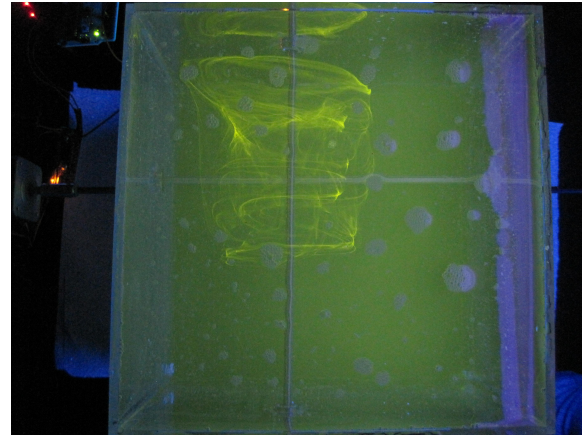


Figure 4.10: A little bit later with $\mu = 10$.

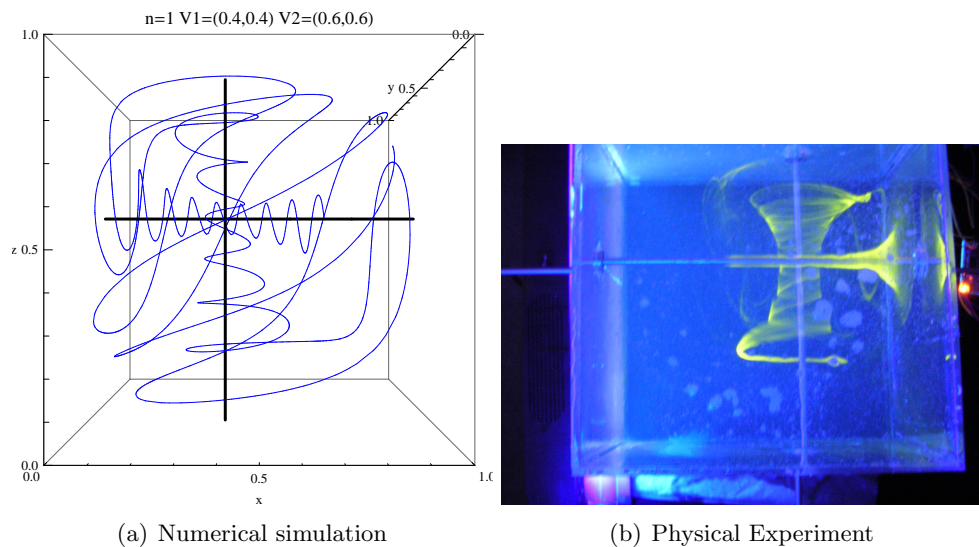


Figure 4.11: A comparison of the numerical simulation and the physical experiment. Notice how in both cases the tracer spirals around the vortex tubes.

Chapter 5

Conclusions

5.1 What This Thesis Did

A foundation has been lain for a blinking vortex-tube model that considers a no-flux, cubic boundary and off-center rolls. Three major components to this model were explored: the analytical development using a lattice of point vortices and the Weierstrass zeta function, the numerical simulation using images of plane-intersections and pathlines, and the physical experimentation which used an apparatus that produced images of dye being stretched into different formations.

The simulations showed evidence that in certain situations, the structure of the flow would break down, and that chaos might exist. This would mean regions of the cube could be *well-mixed*. The physical experiments, while not completely giving results identical to the simulations, showed some similarities. The flow appeared to spend a lot of time spiraling around the rods. Furthermore, although the dye did not appear to form the tori that showed up in the simulation, it did have “holes” near the rods that it rarely entered (see figure 4.9).

5.2 What I Would Do Differently

The biggest change I would make is to the physical apparatus. It would be much better if there was a drainage valve that allowed the glycerin to easily flow out into a bucket. In its current form, the entire apparatus must be lifted and turned upside down

to pour the glycerin out, which is very messy. Also, after each experiment, the dye is mixed with the glycerin, making the tracer in the next experiment harder to see. It would be nice if there was a different kind of tracer (like small beads) that could be filtered out and reused.

The simulation is very computationally expensive. Each time a simulation was run, it took on the order of several hours to complete the process. If the code had been written in a different language, like C, it would most likely be much faster.

5.3 Future Work

Now that the ground work for the model exists, it should be further analyzed. There are a plethora of different schemes that can be created using multiple vortex-tubes. Each scheme can produce different structures in the flow.

While chaos was not explicitly shown to exist, it appeared to arise for larger values of μ . The Lyapunov exponents should be calculated (or approximated) for different regions of the flow.

Bibliography

- [1] Hassan Aref. Stirring by chaotic advection. *J. Fluid Mech.*, 143:1–21, 1984.
- [2] Hassan Aref. The development of chaotic advection. *Physics of Fluids*, 14:1315–1325, 2002.
- [3] Pijush K. Kundu Ira M. Cohen. *Fluid Mechanics*. Academic Press, Burlington, Massachusetts, fourth edition, 2008.
- [4] Mitsuaki Funakoshi. Chaotic mixing and mixing efficiency in a short time. *Fluid Dynamics Research*, 40:1–33, 2008.
- [5] P. Mullowney K. Julien J. D. Meiss. Blinking rolls: Chaotic advection in a three-dimensional flow with an invariant. *SIAM J. Applied Dynamical Systems*, 4:159–186, 2005.
- [6] Kevin A. O’Neil. On the hamiltonian dynamics of vortex lattices. *J. Math. Phys.*, 30:1373–1379, 1989.
- [7] G. O. Fountain D. V. Khakhar I. Mezic J. M. Ottino. Chaotic mixing in a bounded three-dimensional flow. *J. Fluid Mech.*, 417:265–301, 2000.
- [8] Steven H. Strogatz. *Nonlinear Dynamics and Chaos*. Perseus Books Publishing, Cambridge, Massachusetts, 1994.
- [9] J. Chaiken R. Chevray M. Tabor Q. M. Tan. Experimental study of lagrangian turbulence in a stokes flow. *Proceedings of the Royal Society of London. Series A, Mathematical and Physical Sciences*, 408:165–174, 1986.

Appendix A

Simulation Code

A.1 Plane-Intersection

Mathematica code to compute the plane-intersection images (figures 3.2, 3.3, 3.4 and 3.5):

```
SetDirectory[ "C:\\Documents_and_Settings\\Joe\\Desktop\\Thesis_Work\\3D_Simulation\\Plane" ];
Recognizable String
uniqueString = "T=0.0025HighRes";
Number of Points
n = 1;

Initial Location of Points
ptCenter = 1/2;
maxDist = 0;
ptLoc = RandomReal[{ptCenter - maxDist, ptCenter + maxDist}, {n, 3}];

Location of Plane (in y direction)
myPlaneLoc = 1/2;

Location of Vortices
aVortex1 = 2/5;
bVortex1 = 2/5;
aVortex2 = 3/5;
bVortex2 = 3/5;
vLine1 = Line[{{aVortex1, bVortex1, 0}, {aVortex1, bVortex1, 1}}];
vLine2 = Line[{{0, bVortex2, aVortex2}, {1, bVortex2, aVortex2}}];

Duration of Vortices
durVortex1 = 0.0025;
durVortex2 = 0.0025;
```

```

Number of Periods
numPer = 100000;

Velocity Field Calculations
w' = Compile[{ {x, _Real}, {y, _Real}, {\[CapitalGamma], _Real}, {a,
    _Real}, {b, _Real} }, (\[CapitalGamma]/2/Pi/I)*(WeierstrassZeta
[(x+I*y)-(a+I*b), WeierstrassInvariants[{1, I}]] -
WeierstrassZeta[(x+I*y)-(2-a+I*b), WeierstrassInvariants[{1, I}]] +
WeierstrassZeta[(x+I*y)-(2-a+I*(2-b)),
WeierstrassInvariants[{1, I}]] - WeierstrassZeta[(x+I*y)-(a+I
*(2-b)), WeierstrassInvariants[{1, I}]] )];
u = Compile[{ {x, _Real}, {y, _Real}, {\[CapitalGamma], _Real}, {a,
    _Real}, {b, _Real} }, Re[w'[x, y, \[CapitalGamma], a, b]]];
v = Compile[{ {x, _Real}, {y, _Real}, {\[CapitalGamma], _Real}, {a,
    _Real}, {b, _Real} }, -Im[w'[x, y, \[CapitalGamma], a, b]]];

Integrate Velocity Field to Find Streamlines
myList=Table[{}, {n}];
myTable=Table[{}, {0}];
oldYLoc=Table[{}, {n}];
myLabel = StringJoin["n=", ToString[n], "V1=", ToString[aVortex1
//N], ", ", ToString[bVortex1//N], "]V2=", ToString[aVortex2//N
], ", ", ToString[bVortex2//N], "]T1=", ToString[durVortex1//N],
"]T2=", ToString[durVortex2//N]];
For[j=1, j<=2*numPer, j++,
  If[OddQ[j]==True,
    For[i=1, i<=n, i++,
      s[i] = NDSolve[{x'[t]==u[x[t], y[t], 2*Pi
          , aVortex1, bVortex1], y'[t]==v[x[t], y
          t], 2*Pi, aVortex1, bVortex1], z'[t]==0,
          x[0]==ptLoc[[i, 1]], y[0]==ptLoc[[i
          , 2]], z[0]==ptLoc[[i, 3]]}, {x, y, z}, {t
          , 0, durVortex1}];
      myList[[i]]={x[t], y[t], z[t]}/.s[i];
      oldYLoc[[i]]=ptLoc[[i, 2]];
      ptLoc[[i, 1]]=myList[[i, 1, 1]]/.t->
          durVortex1;
      ptLoc[[i, 2]]=myList[[i, 1, 2]]/.t->
          durVortex1;
      ptLoc[[i, 3]]=myList[[i, 1, 3]]/.t->
          durVortex1;
      If[(oldYLoc[[i]]-myPlaneLoc)*(ptLoc[[i
          , 2]]-myPlaneLoc)<0,
        tSoln = FindRoot[{myList
          [[1, 1, 2]]/.t->myVar]==
          myPlaneLoc, {myVar, durVortex1
          /2}]][[1]];
      ]
    ]
  ]
]

```



```

Export Plane
myPlanePlot = Show[myTable]
Export [ StringJoin [ " fifthVortex" , ToString [ aVortex1*5] , ToString
    [ bVortex1*5] , ToString [ aVortex2*5] , ToString [ bVortex2*5] , " "
    Path" , uniqueString , ".pdf" ] , myPlanePlot]

```

A.2 Particle Trajectory

Mathematica code for plotting the trajectory of a particle (figures 3.6 and 3.7):

```

SetDirectory [ "C:\Documents_and_Settings\Joe\Desktop\Thesis\Work
    \3D_Simulation\Path\Torus01Images" ];
Recognizable String
uniqueString = "T=0.010Torus(0.2,0.5,0.4)Rotation";
Number of Points
n = 1;

Initial Location of Points
ptCenter = 1/2;
maxDist = 0;
ptLoc = RandomReal[ { ptCenter - maxDist , ptCenter + maxDist } , { n
    , 3 } ];
ptLoc = { { 0.2 , 0.5 , 0.4 } };

Location of Vortices
aVortex1 = 2/5;
bVortex1 = 2/5;
aVortex2 = 3/5;
bVortex2 = 3/5;
vLine1 = Line [ { { aVortex1 , bVortex1 , 0 } , { aVortex1 , bVortex1 , 1 } } ];
vLine2 = Line [ { { 0 , bVortex2 , aVortex2 } , { 1 , bVortex2 , aVortex2 } } ];

Duration of Vortices
durVortex1 = 0.01;
durVortex2 = 0.01;

Number of Periods
numPer = 2000;

Velocity Field Calculations
w' = Compile [ { { x , _Real } , { y , _Real } , { \[CapitalGamma] , _Real } , { a ,
    _Real } , { b , _Real } } , ( \[CapitalGamma]/2/\bPi/I)*(WeierstrassZeta
    [ (x+I*y)-(a+I*b) , WeierstrassInvariants [ { 1 , I } ] ] -
    WeierstrassZeta [ (x+I*y)-(2-a+I*b) , WeierstrassInvariants [ { 1 , I
    } ] ] + WeierstrassZeta [ (x+I*y)-(2-a+I*(2-b)) ,

```

```

WeierstrassInvariants[{1,I}]] - WeierstrassZeta[(x+I*y)-(a+I
*(2-b)),WeierstrassInvariants[{1,I}]]];

u = Compile[{{x,_Real},{y,_Real},{\[CapitalGamma],_Real},{a,
_Real},{b,_Real}},Re[w'[x,y,\[CapitalGamma],a,b]]];
v = Compile[{{x,_Real},{y,_Real},{\[CapitalGamma],_Real},{a,
_Real},{b,_Real}},-Im[w'[x,y,\[CapitalGamma],a,b]]];

Integrate Velocity Field to Find Streamlines
myList=Table[{}, {n}];
myTable=Table[{}, {0}];
myLabel = StringJoin["n=", ToString[n], "V1=", ToString[aVortex1
//N], ", ", ToString[bVortex1//N], ", ")V2=(", ToString[aVortex2//N
], ", ", ToString[bVortex2//N], ", ")T1=", ToString[durVortex1//N],
" T2=", ToString[durVortex2//N]];
For[j=1,j<=2*numPer,j++,
If[OddQ[j]==True,
For[i=1,i<=n,i++,
s[i] = NDSolve[{x'[t]==u[x[t],y[t],2*\[Pi
,aVortex1,bVortex1],y'[t]==v[x[t],y[
t],2*\[Pi,aVortex1,bVortex1],z'[t]==0,
x[0]==ptLoc[[i,1]],y[0]==ptLoc[[i
,2]],z[0]==ptLoc[[i,3]]},{x,y,z},{t
,0,durVortex1}];

myList[[i]]={x[t],y[t],z[t]}/.s[i];
ptLoc[[i,1]]=myList[[i,1,1]]/.t->
durVortex1;
ptLoc[[i,2]]=myList[[i,1,2]]/.t->
durVortex1;
ptLoc[[i,3]]=myList[[i,1,3]]/.t->
durVortex1;

];
myTable = Join[myTable,Table[ParametricPlot3D[
Evaluate[myList/.t->x],{x,0,durVortex1},
PlotRange->{{0,1},{0,1},{0,1}},AxesLabel->{"x",
"y","z"},PlotLabel->myLabel,
PerformanceGoal->{"Speed"}],{1}]];
];

If[EvenQ[j]==True,
For[i=1,i<=n,i++,
s[i] = NDSolve[{x'[t]==0,y'[t]==v[z[t],
y[t],2*\[Pi],aVortex2,bVortex2],z'[t]==
u[z[t],y[t],2*\[Pi],aVortex2,bVortex2],z
[0]==ptLoc[[i,1]],y[0]==ptLoc[[i
,2]],z[0]==ptLoc[[i,3]]},{x,y,z},{t
,0,durVortex2}]];
]
]
```

```

myList [[ i ]]= {x [ t ] ,y [ t ] ,z [ t ] } /. s [ i ];
ptLoc [[ i ,1]] = myList [[ i ,1 ,1]] /. t ->
    durVortex2 ;
ptLoc [[ i ,2]] = myList [[ i ,1 ,2]] /. t ->
    durVortex2 ;
ptLoc [[ i ,3]] = myList [[ i ,1 ,3]] /. t ->
    durVortex2 ;
];
myTable = Join [myTable , Table [ ParametricPlot3D [
    Evaluate [ myList /. t ->x ] , {x ,0 ,durVortex2 } ,
    PlotRange ->{{0,1},{0,1},{0,1}} , AxesLabel->{"x" , "y" , "z" } , PlotLabel->myLabel ,
    PerformanceGoal->{"Speed"} ] , {1} ] ]
];
Export Animation as .swf File
myPath = Show[myTable , Graphics3D[{ Thick , vLine1 }], Graphics3D
    [{ Thick , vLine2 }]]

```

Appendix B

Microcontroller Code

Arduino code for controlling the rods on the physical experiment:

```
//AUTHOR: Joe Adams
//DATE: February 26, 2010

//SET THESE VARIABLES
///////////////////////////////
double rpms = 180; // sets the angular velocity in rotations
                     per minute
double mu = 10;      // set the value of mu, the nondimensional
                     parameter (\ref{eqn:numMu})
int numIts = 100;    // set the number of iterations to run the
                     experiment
int numTries = 0;    // boolean variable used to make arduino
                     run only once. set equal to zero when done with experiment.
                     set equal to one when ready to use.
int continuous = 0;  // equal to 1 for continuous case, 0
                     otherwise
///////////////////////////////

//initial variables
int dirnVortex1 = 2; // sets vortex 1 direction pin to 2
int stepVortex1 = 3; // sets vortex 1 step pin to 3
int dirnVortex2 = 6; // sets vortex 2 direction pin to 12
int stepVortex2 = 7; // sets vortex 2 step pin to 13
double rodRadius = 2.5; //radius of the rods in mm
double tankLength = 8; //length of side of tank in inch
double stepDelay = (600000)/(16*rpms);
double periodDelay = 30*mu/rpms;
```

```

int x = 0;                                // defines the counter for the
                                             for loop

// calculate the period from the input mu.
double stirPeriod = 100; //seconds

void setup(){
    pinMode(dirnVortex1, OUTPUT); // makes dirnVortex1 pin an
                                   output
    pinMode(stepVortex1, OUTPUT); // makes stepVortex1 pin an
                                   output
    pinMode(dirnVortex2, OUTPUT); // makes dirnVortex2 pin an
                                   output
    pinMode(stepVortex2, OUTPUT); // makes stepVortex2 pin an
                                   output
} // end function setup

void loop(){
    //for continuous stirring
    if(continuous==1){
        digitalWrite(dirnVortex1, LOW);
        digitalWrite(dirnVortex2, LOW);
        delay(100);
        while(numTries==0){
            digitalWrite(stepVortex1, LOW);
            digitalWrite(stepVortex1, HIGH);
            digitalWrite(stepVortex2, LOW);
            digitalWrite(stepVortex2, HIGH);
            delayMicroseconds(stepDelay);
        } //end while
    } //end if

    if(continuous==0){
        int i;
        digitalWrite(dirnVortex1, LOW);
        digitalWrite(dirnVortex2, LOW);
        delay(100);
        while(numTries==0){
            for(i=0;i<=800*mu; i++){
                digitalWrite(stepVortex1, LOW);
                digitalWrite(stepVortex1, HIGH);
                delayMicroseconds(stepDelay);
            } //end for
            for(i=0;i<=800*mu; i++){
        }
    }
}

```

```
    digitalWrite(stepVortex2, LOW);
    digitalWrite(stepVortex2, HIGH);
    delayMicroseconds(stepDelay);
} // end for

} // end while
} // end if
} // end function loop
```